High resolution diffraction imaging for reliable interpretation of fracture systems

B. de Ribet[1*], G. Yelin[1], Y. Serfaty[1], D. Chase[1], R. Kelvin[2] and Z. Koren[1]

Abstract

Small-scale subsurface features, such as natural fractures, act as scattering sources for seismic waves propagating through the subsurface. The wavefield generated by those source points is identified as diffraction energy. The amplitude of this type of energy is much smaller than the recorded events reflected from actual interfaces between different geological layers. Moreover, diffraction energy is normally suppressed by conventional processing and standard imaging algorithms, where summations and averaging processes are applied. The common objective in such processing workflows is to focus on the high specular amplitudes in order to enhance the continuity of seismic reflection events for improving the structural mapping of the subsurface. Our goal is to complement the traditional seismic interpretation workflow by integrating information relative to diffraction energy as another seismic attribute to be interpreted.

The technique applied in this paper is based on a depth imaging algorithm that maps and bins the recorded surface information into multi-dimensional, local angle domain (LAD) common image gathers. The advantage of this system is its unique ability to decompose the wavefield into reflection and diffraction energy directly at the image locations. This paper provides a brief overview of the technology and illustrates its benefits when applied to the Eagle Ford and Barnett shale reservoirs, where seismic data can be of moderate quality, leading to accurate, high-resolution, and high-certainty seismic interpretation for risk-managed field development.

Introduction

Diffraction imaging has proven to be an attractive approach for providing high-resolution subsurface images containing different types and scales of discontinuous geometrical objects. Diffraction imaging in the prestack time domain has been extensively studied (e.g., Khaidukov et al., 2004; Shtivelman and Keydar, 2005; Fomel et al., 2006; Berkovitch et al., 2009 and others). Kozlov et al. (2004) presented diffraction imaging in depth using a 'side wave' Kirchhoff-type migration, where the migration aperture was tapered to filter out the specular energy. Moser and Howard (2008) presented the implementation of diffraction imaging in depth for 2D models, providing a comprehensive review of and insight into the potential of diffracted waves to obtain high-resolution images of small-scale discontinuous subsurface objects. Reshef et al. (2009) showed the application of diffraction energy within dip gathers for high-resolution velocity analysis, especially in areas containing discontinuous objects or along irregular interfaces. Koren et al. (2008), Koren and Ravve (2010), and in particular Koren and Ravve (2011), described a novel imaging method which is based on the ability to decompose the full recorded seismic wavefield into continuous full-azimuth directivity components in situ at the subsurface image points. The proposed method follows the concept of imaging and analysis in the 'Local Angle Domain (LAD)'. Further implementations and enhancements of this method have been presented by Inozemtsev et al. (2013), Kowalski et al. (2014), Konyushenko et al. (2014), Inozemtsev et al. (2015) and Chase and Koren (2016). Benfield et al. (2016) showed the feasibility of integration of the LAD approach into the full interpretation workflow by demonstrating the practicality of automatic fault extraction based on the extracted diffraction information.

The work presented in this paper is a continuation of the above studies. We show the power of this system in obtaining high-resolution, small discontinuous objects, such as fracture systems, in the Eagle Ford and Barnett unconventional shale plays.

Method

The proposed method follows the concept of imaging and analysis in the Local Angle Domain (LAD). Using an asymptotic ray-based migration/inversion 'point-diffractor' operator, ray paths, slowness vectors, traveltimes, geometrical spreading and phase rotation factors are calculated from the subsurface image points up to the surface, forming a system for mapping (migrating) the recorded surface seismic data into the image points. Concurrently, the amplitude preserved migrated events are decomposed (binned) and stored in multi-dimensional LAD common image gathers. The primary objective of this huge multi-dimensional angle domain decomposition is to provide a platform for evaluating the amplitude contribution of each individual ray pair (incident and scattered waves at the 'reflection/diffraction'

[1] Paradigm | [2] Seitel

[*] Corresponding author, E-mail: Bruno.deRibet@PDGM.com

points) into the total migrated image. The directivity (dip and azimuth) of the ray pairs is measured as the vector sum of their individual incident and scattered slowness vectors. The amplitude of the ray pairs scattered from points in the vicinity of actual subsurface reflectors, in which their directivity is more or less collinear with the normal direction of the subsurface reflectors, is associated with 'specular waves'. These carry much higher energy than all other non-specular (referred here as diffraction) waves. Moreover, the distribution of the specular energy along the 3D directional gathers has a certain concave surface shape (formulated and displayed for 3D homogeneous media in Koren and Ravve, 2010), where the higher amplitudes occur at the base (small horizontal patch) of this specular surface. This fact makes it possible to design a special specularity measure (attribute) in each ray pair direction in the LAD CIGs, accounting for both the energy and the coherence along the computed concave surfaces. The specularity measures are performed in local windows around the individual depth points and directivity bins within the directional LAD gathers. The specularity attributes are then used as weighted stack filter components, providing the ability to decompose the specular and diffraction energy from the total scattered field obtained in the full-azimuth directional angle gathers, which is the core component of our imaging system.

Two types of images are constructed: Specular weighted stacks for emphasizing subsurface structure continuity, and diffraction weighted stacks, which emphasize discontinuities in small-scale objects such as faults, channels and fracture systems. Note that full-azimuth directional angle decomposition does not necessarily require a wide-azimuth acquisition geometry system. However, a large migration aperture is needed to allow information from all directions. Moreover, in many cases it is sufficient to use small offsets to create directional angle gathers. For example, it has been shown that nearly vertical faults and salt flanks can be detected via simulated corner (duplex) waves established with directional angle decomposition, where the integration is performed on narrow opening angles (narrow cones) only (Kozlov et al., 2008). The powerful blending of the two different types of images, specular and diffracted, into a single image was demonstrated in Benfield et al. (2016).

Case studies

Eagle Ford Shale – South Texas

The Eagle Ford Shale deposition occurred 90 million years ago on top of the Woodbine group in South and East Texas. It is the source rock for the overlying conventional Austin Chalk oil and gas reservoir. The reservoir unit within this formation is actually more carbonate than shale, with only around 30% clay present. The higher percentage of carbonate increases its brittleness, which suggests it is more favourable for hydraulic fracturing. Oil reserves alone have been estimated in the range of 5 to 20 billion barrels.

Figure 1 shows the resolution of diffraction energy, where high energy reflections from flat events have been removed. Energy from reflections is significantly stronger than diffraction energy: therefore, energy scattered from edge diffractions or corner waves at the fault location is masked by the strong reflection

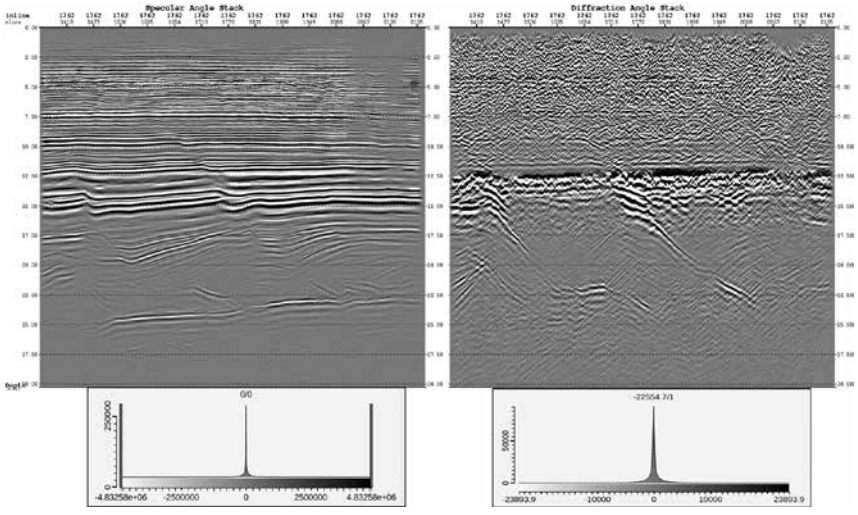

Figure 1 Specular reflection stack (left) and diffraction stack (right) with their respective value ranges (data courtesy of Seitel).

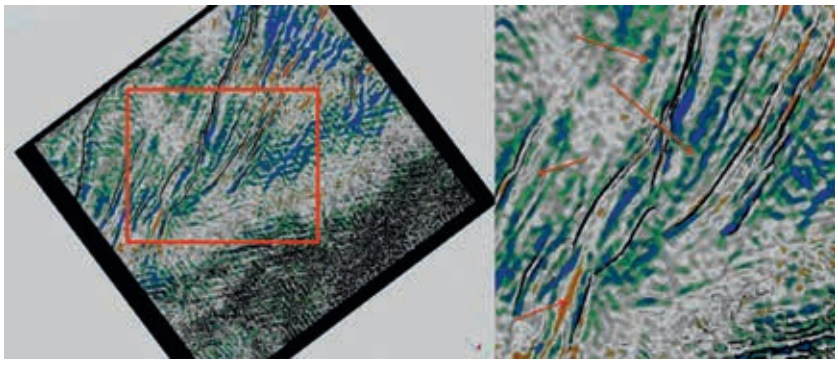

Figure 2 Depth slice, merge of extracted diffraction and coherence volumes. Enlarged area corresponds to red square. Red arrows indicate improvements in the fault definition (continuity, extension and potential) (data courtesy of Seitel).

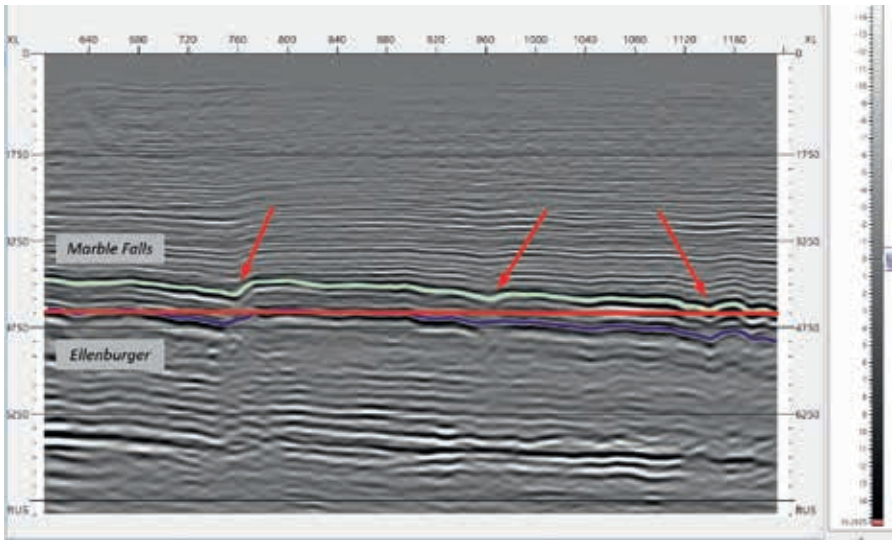

Figure 3 Specular reflection stack with interpreted seismic events (Marble Falls and Ellenburger). The red horizontal line at 1372 m is the reference for further analysis.

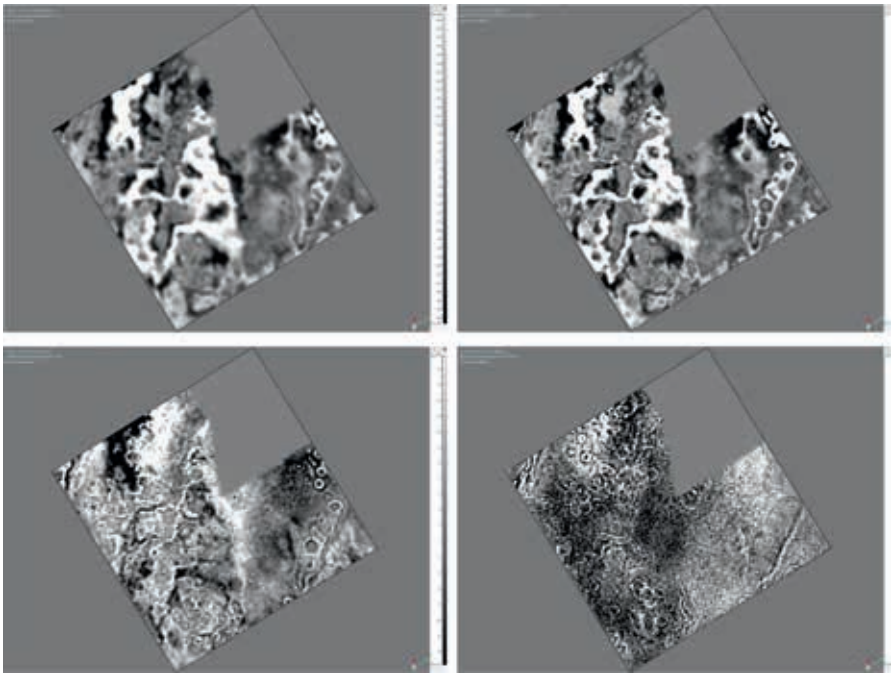

Figure 4 Depth slice 1372 m, different ranges of dip were stacked. As we separate reflections from diffraction energy, karsts and faults are revealed with higher resolution. From upper left to lower right: all dips stacked (0°-45°), 0°-15°, 15°-30°, 30°-45°.

energy (left image). The image on the right shows a diffraction stack upon removal of the reflection energy. Fault lineaments are clearly highlighted and present better continuity.

Natural fractures in shale formations can provide a pathway for higher permeability; therefore, they need to be characterized. Geometrical attributes such as coherence are commonly used for mapping fault/fracture lineaments. The most appropriate process for reviewing diffraction volume results is to compare them with geometrical attributes from conventional poststack attributes. To understand the benefit of interpreting the diffraction volume along with other poststack seismic attributes, an extraction of both attributes on to a depth slice at the depth of the zone of interest, and merged into a single view, represents a good approach in the case of the Eagle Ford. It is clear that more continuous lineaments are visible on the diffraction volume (Figure 2, red to blue palette) than on the coherence volume (Figure 2, black and white palette). The position and trend of fault lineaments are consistent between the two attributes. Fault lineaments can be extended (Figure 2) using the diffraction volume, which in this case was generated by applying energy weights during the stacking process. New potential fault lineaments (Figure 2) are visible on the extracted diffraction attribute depth slice, which allows the interpretation of a high-definition structural pattern at the limits of the seismic vertical resolution.

Barnett Shale – Fort Worth Basin

The Barnett Shale formation was laid down in the Fort Worth Basin 350 million years ago. The reservoir within this formation is not considered true shale because of its highly variable mineral composition, which is dominated by large percentages of silica. The mineralogy lends itself to increased brittleness, which has resulted in a naturally fractured reservoir. Gas reserves from 5 to 30 trillion cubic feet have been estimated in the Barnett, along with almost 100 million barrels of oil and a potential 1.1 billion

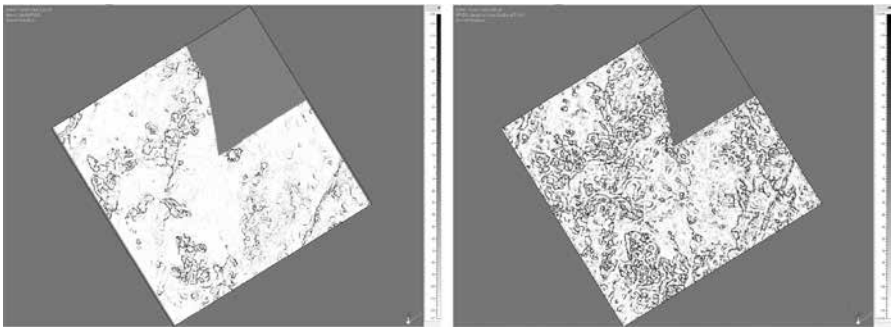

Figure 5 Depth slice 1372 m, high-resolution Eigen-based coherence from existing specular reflection stack (left) and from the 15°-30° dip stacking range (right).

barrels of condensate. Producing hydrocarbons in a karsted and fractured reservoir has always been a high-risk procedure. This is the case in the Barnett Shale, known as a tight gas reservoir, which implies the necessity of a major hydraulic fracturing effort to produce from this formation. The Barnett Shale overlies the karsted and fractured aquifer limestone of the Ellenburger Group. Even if oil and gas companies have learnt how to effectively position a horizontal well and frack the reservoir, the success of a well completion needs to take into account the risk of connecting the Ellenburger formation, through faults and karsts, with water.

Figure 3 illustrates the characteristics of the seismic data on a vertical seismic section, considering a full wavefield stack. The presence of natural karst-related collapse chimneys is known in this region, with larger structural collapses visible on auto-tracked seismic horizons. The location of those collapses (Figure 3, red arrows) clearly corresponds to a pull-down of the seismic events. Any structural and stratigraphic interpretation at the depth of the Barnett Shale formation requires high-resolution images of the area in order to map the presence of major faults and karsts. However, detailed mapping of these features requires additional attribute analysis. For example, curvature volumes have proven to be useful for identifying the location and extent of the collapsed chimneys, with the largest response at the core of these features. Meanwhile, coherence blended with amplitude will help to determine the vertical extension of faults, the circumference of the collapsed chimneys with greatest vertical change, and eventually more subtle geological features.

In the example below (Figure 4), we show that the use of high-resolution diffraction images benefits the seismic interpretation in order to accurately map the presence of faults and to delineate the extension of the karsts (see also Grasmueck, 2012). In this case, different ranges of apparent dips were tested for the final stack image. The idea was to separate the strong energy of the primary reflections at low dips from the secondary reflections and diffractions at higher dips, where the energy is lower and masked by the high energy of the primary reflections, particularly in the vicinity of the karsts. Figure 4 shows the same depth slice at the karst depth level. Stacks were generated for four different dip ranges: 0°-15°, 15°-30°, 30°-45° and 0°-45° (all dips) which we associate with the full wavefield stack.

At 1372 m, which corresponds approximatively to the Barnett Shale formation depth, the diffraction volumes highlight the faults and collapsed chimneys differently (Figure 4); the most precise or highest resolution is associated with the dip stacking range of 15°-30°. This approach can be validated by generating attributes from the best image that clearly would reveal the benefits of the partial stacking method, to be compared with the same seismic attribute created from the full wavefield. As the coherence attribute is a proven seismic attribute for delineation, because of the vertical changes occurring in the vicinity of the collapsed chimneys and faults, it represents the most appropriate method for comparison. After generation of the coherence volume, the seismic coherence attributes have been extracted along the same depth slice (1372 m).

Both images (Figure 5) show a similar pattern that indicates the presence and distribution of major faults and karsts. However, more details are revealed on the structural attribute generated

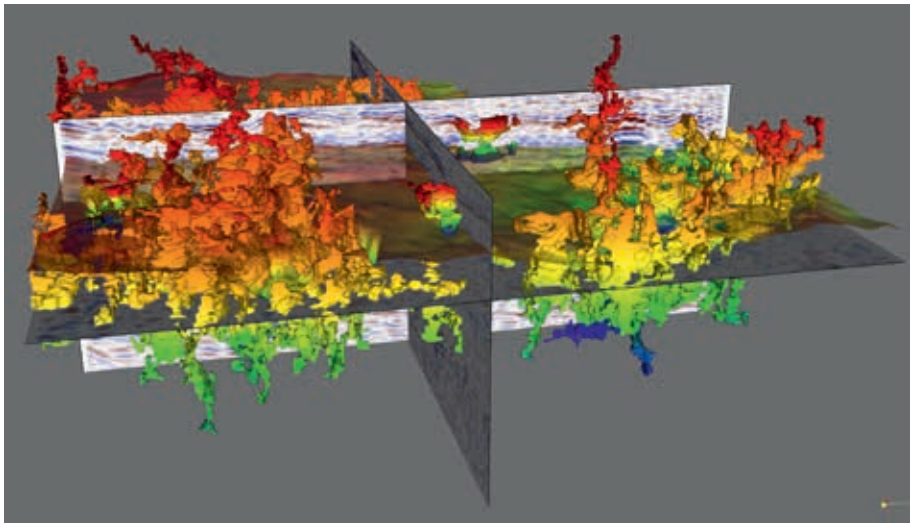

Figure 6 Detected complex geobodies (from curvature attribute generated from 15°-30° partial dip stacking) corresponding to karst features, jointly visualized with diffracted stack attribute and top of the Ellenburger formation (semi-transparency).

from the partial stacked attribute. In the left image, a few collapsed chimneys have been identified and it can be observed that they are located in specific areas without visible connection between each 'cluster' from this depth slice. In the image on the right (15°-30° dip stacking), the distribution is similar with a higher degree of detail, which seems to confirm the connection between different types of faulted clusters.

High-definition delineation is now possible, with the ability to directly integrate derived seismic attributes from the partial stacking method in a conventional seismic interpretation workflow.

Volume interpretation can be performed to map the collapsed chimneys in three dimensions. The extraction of multi-Z value surfaces shows details about their extension. These features are not only present in the zone of interest (Barnett Shale formation), but extend above the Marble Falls and below the Ellenburger (Figure 6), often intersecting with fault planes and extending the area of permeability risk, as they would act as a preferred migration path for water.

Conclusion

Two field examples were used to demonstrate the applicability of diffraction imaging of prestack data to generating high-resolution seismic images that allow the interpretation of small-scale discontinuous objects with more confidence. The results are compared with the conventional poststack approach, which is designed to increase resolution and delineate geological features by computing geometrical attributes like coherence and curvature. The comparison clearly shows the superior resolution obtained by the migrated diffraction stack images over the coherence and/or curvature attribute images. Further improvements can be achieved when the two approaches are combined by computing the coherence/curvature attributes over previously generated diffraction stack images.

Acknowledgments

The authors would like to thank Paradigm for permission to publish and present this work, and Seitel for permission to use the Eagle Ford seismic data.

References

Benfield, N., Guise, A. and Chase, D. [2016]. Diffraction imaging – a tool to reduce exploration and development risk. *First Break*, **34**, 57-63.

Berkovitch, A., Belfer, I., Hassin, Y. and Landa, E. [2009]. Diffraction Imaging by Multifocusing. *Geophysics*, **74** (6), WCA75-WCA81.

Chase, D. and Koren, Z. [2015]. 5D Local Angle Domain Gathers as an ideal representation for directivity driven imaging. *77th EAGE Conference and Exhibition,* Extended Abstracts, WS12-B02.

Fomel, S., Landa, E. and Taner, M.T. [2006]. Post-stack velocity analysis by separation and imaging of seismic diffractions. *76th SEG Exposition and Annual International Meeting*, Expanded Abstracts, 2559-2563a.

Grasmueck, M., Moser, T.J., Pelissier, M.A., Pajchel, J. and Pomar, K. [2015]. Diffraction signatures of fracture intersections, *Interpretation*, **3**, SF55-SF68.

Inovemstev, A., Nicolaevich, S., Viktorovich, I., Galkin, A., Vasilyevich, R. and Koren, Z. [2013]. Applying full–azimuth angle domain prestack migration and AVAZ inversion to study fractures in carbonate reservoirs in the Russian Middle Volga region. *First Break*, **31**, 79-83.

Inozemtsev, A., Koren, Z. and Zapprikaspiygeofizika, G. [2015]. Noise suppression and multiple attenuation using full-azimuth angle domain imaging: case studies. *First Break*, **33**, 81-86.

Khaidukov, V., Landa, E. and Moser, T.J. [2004]. Diffraction imaging by focusing-defocusing: An outlook on seismic superresolution. *Geophysics*, **69**, 1478-1490.

Konyushenko, A., Shumilyak, V., Solgan, V., Inozemtsev, A., Solovyev, V. and Koren, Z. [2014]. Using full-azimuth imaging and inversion in a Belarus salt dome tectonic regime to analyze fracturing in Upper Devonian intersalt and subsalt carbonate reservoirs. *First Break*, **32**, 81-88.

Koren, Z., Ravve, I., Ragoza, E., Bartana, A. and Kosloff, D. [2008]. Full-azimuth angle domain imaging. *78th SEG Exposition and Annual International Meeting*, Expanded Abstracts.

Koren Z. and Ravve, I. [2010]. Specular/diffraction imaging by full azimuth subsurface angle domain decomposition. *80th SEG Exposition and Annual International Meeting,* Expanded Abstracts.

Koren Z. and Ravve I. [2011]. Full azimuth subsurface angle domain wavefield decomposition and imaging Part 1 and 2. *Geophysics,* **76** (1-2).

Kowalski, H., Godlewski, P., Kobusinski, W., Makarewicz, W., Podolak, M., Nowicka, A., Mikolajewski, Z., Chase, D., Dafni, R., Canning, A. and Koren, Z. [2014]. Imaging and characterization of a shale reservoir onshore Poland, using full-azimuth seismic depth imaging. *First Break*, **32** (10), 101-109.

Kozlov, E., Barasky, N., Korolev, E., Antonenko, A. and Koshchuk, E. [2004]. Imaging scattering objects masked by specular reflections. *74th SEG Exposition and Annual International Meeting*, Expanded Abstracts.

Kozlov, E.A., Koren, Z., Tverdohlebov, D.N., and Badeikin, A.N. [2009]. Corner reflectors – a new concept of imaging vertical boundaries. *71st EAGE Conference and Exhibition*, Extended Abstracts, Z039.

Moser, T.J. and Howard, C.B. [2008]. Diffraction imaging in depth. *Geophysical Prospecting*, **56**, 627-641.

Reshef, M., Lipzer, N. and Landa, E. [2009]. Interval velocity analysis in complex areas – azimuth considerations. *71st EAGE Conference and Exhibition*, Extended Abstracts, U010.

Shtivelman, V. and Keydar, S. [2005]. Imaging shallow subsurface inhomogeneities by 3D multipath diffraction summation. *First Break*, **23**, 39-42.

Doi: 10.3997/1365-2397.2017003